Reachable-set characterization of an open quantum system by the quantum speed limit

Kohei Kobayashi
Quantum Computing Center, Keio University, Hiyoshi 3-14-1, Kohoku, Yokohama 223-8522, Japan

(Received 8 November 2021; accepted 29 March 2022; published 18 April 2022)

In recent years, the idea of reachable-set characterization based on the quantum speed limit (QSL) was proposed by Arenz *et al.* [New J. Phys. **19**, 103015 (2017)]; that is, the reachable set of the target unitary gate in a closed qubit system can be characterized by considering the QSL as the necessary condition that the control setup must satisfy in order to achieve the goal. Inspired by this idea, in this paper we characterize a general Markovian open quantum system based on the QSL derived by Kobayashi and Yamamoto [Phys. Rev. A **102**, 042606 (2020)]. Note that this bound is not only explicitly computable with respect to system parameters but also tighter than the other bounds. Some examples for demonstrating this analysis will be given.

DOI: 10.1103/PhysRevA.105.042608

I. INTRODUCTION

Quantum information technologies, e.g., quantum computing, communication, teleportation, and metrology, have received a lot of attention in recent years due to their possibility to outperform classical information processing. These technologies are described by a sequence of qubits for an information resource. Therefore, a technique of quantum control which efficiently and accurately prepares the desired quantum states plays an important role. However, in the practical situation, there is an undesirable environment effect such as *decoherence* which destroys the coherence properties of quantum systems, resulting in the actual control performance severely degrading. Thus, it is important to quantitatively evaluate and characterize a reachable set of the controlled state, i.e., the set of all the final states reachable starting from the initial state, from the perspective of quantum engineering. In general, the reachable set is described as a time-dependent function, e.g., Lie-semigroup structures [1], the C-numerical range [2], the spectrum of the density matrix [3], and so on. In order to study this problem, the *quantum speed limit* (QSL) can be a useful tool.

The QSL is defined as a fundamental lower bound on the evolution time of a quantum state from an initial state to a final state. The study of the QSL started with closed systems; Mandelstam and Tamm presented the first QSL between orthogonal states [4], which is bounded by the variance of the system energy. Later, Margolus and Levitin provided another QSL depending on the mean energy [5], and extensions to mixed states [6], nonorthogonal states [7,8], time-dependent driven systems [9,10], and open quantum systems [11–16] have been investigated. The QSL gives a trade-off relation between the control time and energy resource, and thus, it has several applications in quantum control scenarios [17–21]. Actually, the connection between the reachable set and the QSL has been studied in recent years. In Ref. [22] the authors characterized the sets of all target unitary gates by considering the QSL for the control time as the necessary condition that control parameters, e.g., the drift and control Hamiltonians and driving time, must satisfy to implement the target gate.

Inspired by the above facts, in this paper we extend the work given in [22] to general Markovian open quantum systems. More precisely, we characterize the reachable set of an open quantum system under a certain situation, e.g., initial state, Hamiltonian, decoherence, and evolution time, using the QSL. In order to make this analysis tractable and rigorous, we employ the bound derived in [23] because it is not only explicitly computable with respect to control parameters but also tighter than the other explicit bounds. Section III provides some examples for demonstrating this analysis with insightful notions.

II. QUANTUM SPEED LIMIT

A. Setup and derivation

We begin with introducing the QSL presented in [23]. We consider the Markovian master equation

$$\frac{d\rho_t}{dt} = -i[H, \rho_t] + \mathcal{D}[M]\rho_t, \tag{1}$$

where H is the time-independent Hamiltonian. M is the Lindblad operator representing the decoherence, and thus, $\mathcal{D}[M]\rho = M\rho M^\dagger - M^\dagger M\rho/2 - \rho M^\dagger M/2$. Throughout this paper, we assume that $\hbar = 1$ and the initial state is pure, i.e., $\rho_0 = |\psi_0\rangle\langle\psi_0|$. Next, we focus on the relative purity Θ_t between the initial state and the final state,

$$\Theta_t := \arccos(\langle\psi_0|\rho_t|\psi_0\rangle), \tag{2}$$

where $0 \leqslant \Theta_t \leqslant \pi/2$. The relative purity has often been employed to derive the QSL [12,15]. The upper bound is achieved when ρ_0 and ρ_t are orthogonal, and the lower one is achieved only when $\rho_t = \rho_0$. In this setting, we find that the dynamics of Θ_t is upper bounded as follows:

$$\frac{d\Theta_t}{dt} \leqslant \frac{1}{\sin\Theta_t}(\mathcal{A}\sqrt{1-\cos\Theta_t} + \mathcal{E}), \tag{3}$$

with

$$\mathcal{A} = \sqrt{2}\big(\|i[H, \rho_0] + \mathcal{D}^\dagger[M]\rho_0\|_{\mathrm{F}}\big),$$
$$\mathcal{E} = \|M|\psi_0\rangle\|^2 - |\langle\psi_0|M|\psi_0\rangle|^2,$$

where $\|X\|_{\rm F} = \sqrt{{\rm Tr}(X^\dagger X)}$, $\||\psi\rangle\| = \sqrt{\langle\psi|\psi\rangle}$, and $\mathcal{D}^\dagger[M]\rho = M^\dagger\rho M - M^\dagger M\rho/2 - \rho M^\dagger M/2$. Integrating the above inequality (3) from 0 to T, we obtain the following lower bound [23]:

$$T \geqslant T_* := \frac{2\lambda}{\mathcal{A}} + \frac{2\mathcal{E}}{\mathcal{A}^2}\ln\left(\frac{\mathcal{E}}{\mathcal{E}+\mathcal{A}\lambda}\right), \tag{4}$$

with $\lambda = \sqrt{1-\cos\Theta_T}$ $(0 \leqslant \lambda \leqslant 1)$. The derivation of the above results is given in Appendix A. λ is 1 when ρ_t is orthogonal to ρ_0 and is zero only when $\rho_t = \rho_0$. Hence, λ can be interpreted as the radius of the ball around ρ_0. The QSL T_* gives a lower bound on the time T for the state ρ_t to evolve from ρ_0 to ρ_T (i.e., Θ_t evolves from 0 to Θ_T).

As shown in Ref. [23], T_* has the following notable features.

(i) T_* is applicable to a general Markovian open quantum system driven by arbitrary time-independent H and M.

(ii) T_* is explicitly computable once the parameters (ρ_0, H, M, Θ_T) are specified. As a result, it is not necessary to calculate T_* to solve any equations.

(iii) When $M = M^\dagger$, $H = 0$, and $|\psi_0\rangle$ is an eigenstate of M or $M = 0$ and $[H, \rho_0] = 0$, we have $T_* \to \infty$ because $\mathcal{A} = \mathcal{E} = 0$. In this case, the state cannot reach any $\rho_T \neq \rho_0$, resulting in λ remaining zero.

(iv) T_* gives a tighter bound when λ is small. In Appendix B, we show the actual tightness of T_* by comparing T_* with the exact evolution time T.

(v) T_* is tighter than the other explicit bound; for the same setup mentioned above, del Campo provided the lower bound: $T \geqslant T_{\rm DC} := \sqrt{2}\lambda/\mathcal{A}$ [12]. Note that $T_* \geqslant T_{\rm DC}$ holds when the decoherence is small or the radius λ is small.

(vi) If H is time dependent, we cannot generally solve the integral (3). In order to calculate T_*, let us write $H_t = u_t H'$ with the time-dependent control input u_t and fixed H'. Assuming u_t has the constraint $u_{\max} := \max\{|u_t|\}$ and using the triangle inequality, $\mathcal{A}$ is redefined as follows:

$$\mathcal{A}' = \sqrt{2}(u_{\max}\|i[H', \rho_0]\|_{\rm F} + \|\mathcal{D}^\dagger[M]\rho_0\|_{\rm F}). \tag{5}$$

Therefore, in this case the QSL is given by (4) after replacing $\mathcal{A}$ with $\mathcal{A}'$.

B. Reachable-set characterization based on the quantum speed limit

Here we explain the idea of characterization of the reachable set of final states based on the QSL. The parameters determining the state evolution (ρ_0, H, M, T) and the fidelity-based distance λ are correlated via the inequality $T \geqslant T_*$. In other words, this relation can be considered a necessary condition that (ρ_0, H, M, T) must satisfy in order to achieve a certain value of λ. Therefore, once the system's parameters are specified, we can characterize the set of all λ (i.e., all final states $|\psi_T\rangle$) by examining $T \geqslant T_*$.

Here it should be noted that as T or λ increases, the performance of T_* becomes weak. However, when T is short or λ is small, the idea posed above gives useful insight into the practical reachability problem, for example, how close to a target state the controlled state can be steered within a given control time or how long the state can be preserved around an ideal initial state under a given decoherence.

In what follows, some typical examples demonstrating this idea will be given.

III. EXAMPLE

A. Qubit

The first example is a qubit system consisting of the excited state $|0\rangle = [1, 0]^\top$ and the ground state $|1\rangle = [0, 1]^\top$. Its initial pure state can be fully parametrized by the Bloch representation:

$$|\psi_0\rangle = [\cos\theta,\ e^{i\varphi}\sin\theta]^\top, \tag{6}$$

where $0 \leqslant \theta, \varphi \leqslant \pi$. Also the system observables along the i axis $(i = x, y, z)$ are given by the Pauli matrices $\sigma_x = |0\rangle\langle 1| + |1\rangle\langle 0|$, $\sigma_y = -i|0\rangle\langle 1| + i|1\rangle\langle 0|$, and $\sigma_z = |0\rangle\langle 0| - |1\rangle\langle 1|$. Here we consider the following setup:

$$H = \Omega\sigma_z,\ M = \sqrt{\gamma}\sigma_-. \tag{7}$$

H represents the rotation of the state along the z axis with frequency $\Omega > 0$, and M represents the energy decay $|0\rangle \to |1\rangle$ with decay rate $\gamma > 0$. In this case, the lower bound is given by (4) with

$$\mathcal{A} = \sqrt{2\gamma^2\cos^2 2\theta + \left(4\Omega^2 + \frac{\gamma^2}{4}\right)\sin^2 2\theta},$$
$$\mathcal{E} = \gamma\cos^4\theta.$$

First, we focus on the case of $\gamma = 0$, where λ has an upper bound $\lambda \leqslant \Omega|\sin 2\theta|T$. Figure 1(a) shows the reachable set of λ for each initial state and driving time. The colored area shows all sets satisfying this inequality, and the white area shows the one that does not satisfy it. We find that the three curves are zero at $\theta = 0$ and $\pi/2$, meaning that $|0\rangle$ and $|1\rangle$ do not change under the rotation. This is consistent with the fact that $|0\rangle$ and $|1\rangle$ are the steady state of the equation $d\rho_t/dt = -i\Omega[\sigma_z, \rho_t]$. Moreover, the reachable sets are maximum at the superposition $|+\rangle := (|0\rangle + |1\rangle)/\sqrt{2}$. This implies that the rate of the state change from $|+\rangle$ is biggest, and thus, $|+\rangle$ is the most fragile state against the rotation by H.

On the other hand, when $\gamma = 1$, the curves are maximum at $\theta = 0$ [Fig. 1(b)]. This is because $|0\rangle$ is largely affected by the decoherence M, while it is unchanged against H because $|0\rangle$ is the eigenstate of H. In particular, it is noted that the state cannot reach its orthogonal state within $T = 0.1$ or 0.3, while $|\psi_0\rangle$ with $\theta \leqslant 0.9$ may do so within $T = 0.8$.

Next, we consider the state preparation by unitary gates; more specifically, under a given initial state $|\psi_0\rangle$, time-dependent Hamiltonian H_t, and driving time T, we characterize an implementable unitary gate (assume $M = 0$).

Let the target gate be the rotation operator $G(\alpha, \beta, \delta) = R_z(\alpha)R_y(\beta)R_z(\delta)$, with

$$R_z(\alpha) = e^{-i\frac{\alpha}{2}\sigma_z} = \begin{bmatrix} e^{-i\frac{\alpha}{2}} & 0 \\ 0 & e^{i\frac{\alpha}{2}} \end{bmatrix},$$

$$R_y(\beta) = e^{-i\frac{\beta}{2}\sigma_y} = \begin{bmatrix} \cos\frac{\beta}{2} & -\sin\frac{\beta}{2} \\ \sin\frac{\beta}{2} & \cos\frac{\beta}{2} \end{bmatrix},$$

$$R_z(\delta) = e^{-i\frac{\delta}{2}\sigma_z} = \begin{bmatrix} e^{-i\frac{\delta}{2}} & 0 \\ 0 & e^{i\frac{\delta}{2}} \end{bmatrix},$$

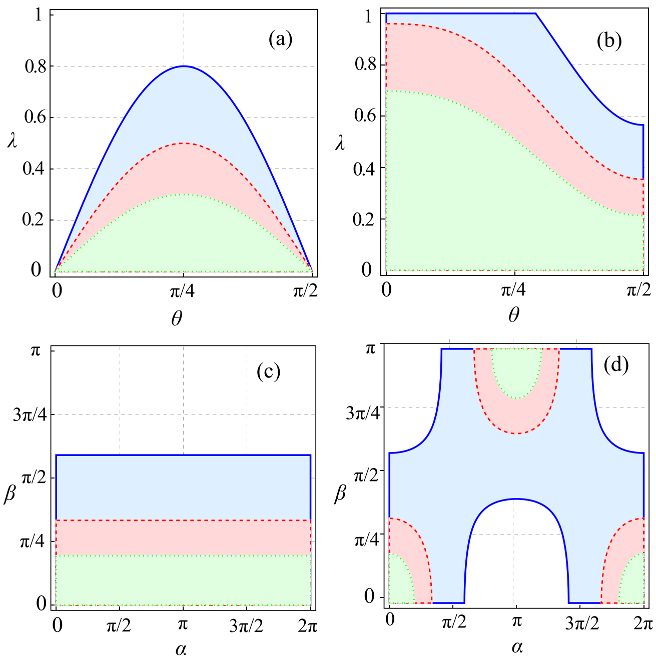

FIG. 1. Reachable set of λ as a function of θ for each evolution times $T = 0.3$ (dotted green line), $T = 0.5$ (dashed red line), and $T = 0.8$ (solid blue line) when (a) $\gamma = 0$ and (b) $\gamma = 1$, in units of $\Omega = 1$. Reachable set of the target gate $G(\alpha, \beta)$ for $T = 0.3$ (dotted green line), $T = 0.5$ (dashed red line), and $T = 0.8$ (solid blue line) when (c) $\theta = 0$ and (d) $\theta = \pi/4$, in units of $\Omega = u_{\max} = 1$.

where $0 \leqslant \alpha < 2\pi$, $0 \leqslant \beta < \pi$, and $0 \leqslant \delta < 4\pi$. R_y and R_z represent the rotation around the y and z axes, respectively, and the transformation from $|\psi_0\rangle$ to $|\psi_T\rangle$ is described as $|\psi_T\rangle = G(\alpha, \beta, \delta)|\psi_0\rangle$. Also we take the Hamiltonian as

$$H_t = \Omega\sigma_x + u_t\sigma_z. \tag{8}$$

Note that the state is fully controllable; hence, every $G(\alpha, \beta) \subset \mathrm{SU}(2)$ can be implemented by suitably choosing u_t for sufficient time [22]. In this case the lower bound is calculated as follows:

$$T_* = \frac{\sqrt{1 - \cos^2\frac{\alpha}{2}\cos^2\frac{\beta}{2} - \sin^2\frac{\alpha}{2}\cos^2\left(2\theta + \frac{\beta}{2}\right)}}{\Omega|\cos 2\theta| + u_{\max}|\sin 2\theta|}. \tag{9}$$

If $\theta = 0$, $T_* = |\sin(\beta/2)|/\Omega$. Figure 1(c) shows the sets that satisfy $T \geqslant T_*$ for $T = 0.3$, 0.5, and 0.8 under fixed $\Omega = u_{\max} = 1$. Note that when $T = 0.5$, this inequality is saturated at $\beta = \pi/3$, where the target is given by

$$G(\alpha) = \frac{1}{2}\begin{bmatrix} \sqrt{3}e^{-i\frac{\alpha}{2}} & -e^{-i\frac{\alpha}{2}} \\ e^{i\frac{\alpha}{2}} & \sqrt{3}e^{i\frac{\alpha}{2}} \end{bmatrix}.$$

This G gives the final fidelity $\cos\Theta_T = 0.75$. Then we can steer the state only to the one with a fidelity of about 0.75 at most in $T = 0.5$. Next, for the case of $\theta = \pi/4$, the lower bound is $T_* = |\sin(\alpha/2 - \beta/2)|/u_{\max}$. Clearly, the reachable sets depicted in Fig. 1(d) are remarkably changed from Fig. 1(c). The lower bound $T_*(\alpha, \beta)$ is zero at $G(0, 0) = G(2\pi, 0) = I$ and $G(\pi, \pi) = i\sigma_x$ because $|\psi_0\rangle = |+\rangle$ is the eigenstate of σ_x. This means that there is no difference between $|\psi_0\rangle$ and $|\psi_T\rangle$ in terms of the fidelity. On the other hand,

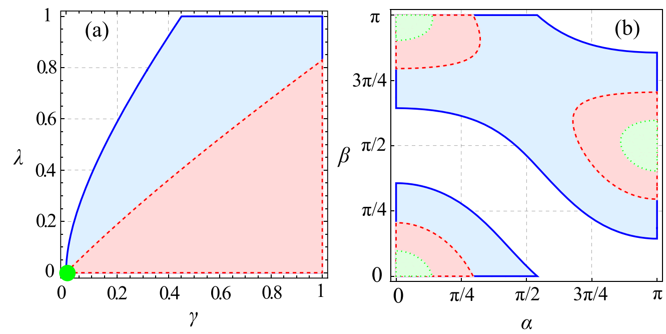

FIG. 2. (a) Reachable sets of λ as a function of γ at $T = 0.5$ when the initial state is $|\Psi^+\rangle$ (solid blue line), $|\Phi^\pm\rangle$ (dashed red line), and $|\Phi^-\rangle$ (green dot at the origin). (b) Reachable set of the target gate $G(\alpha, \beta)$ in units of $\Omega = u_{\max} = 1$ for $T = 0.15$ (dotted green line), $T = 0.30$ (dashed red line), and $T = 0.45$ (solid blue line).

$T_*(\alpha, \beta)$ is maximized at

$$G(0, \pi) = G(2\pi, \pi) = -i\sigma_y, \ \ G(\pi, 0) = i\sigma_z. \tag{10}$$

Actually, these gates cannot be implemented even if $T = 0.8$. Indeed, this result is reasonable because the target final states generated by $-i\sigma_y$ and $i\sigma_z$ are given as $|\psi_T\rangle = (|0\rangle - |1\rangle)/\sqrt{2}$ and $i(|0\rangle - |1\rangle)/\sqrt{2}$, which are orthogonal to $|\psi_0\rangle$. Therefore, we can conclude that it takes longer to prepare the state that is far from $|\psi_0\rangle$. As shown above, by using T_*, we can characterize the set of target states or target gates under a given control setting.

B. Two qubits

Here we study a two-qubit system driven by decoherence. We first consider the Bell states, which are the maximally entangled states defined as

$$|\Phi^\pm\rangle = \frac{1}{\sqrt{2}}(|0\rangle \otimes |0\rangle \pm |1\rangle \otimes |1\rangle),$$

$$|\Psi^\pm\rangle = \frac{1}{\sqrt{2}}(|1\rangle \otimes |0\rangle \pm |0\rangle \otimes |1\rangle).$$

The Bell states are used as a main resource for quantum information processing such as quantum teleportation. Therefore, it is of particular interest to compare the sets of states from each Bell state under undesirable noises. Now we take the collective (global) noise modeled by $M = \sqrt{\gamma}(\sigma_- \otimes I + I \otimes \sigma_-)$. Also for simplicity, we assume $H = 0$. Then, the lower bound for each state is calculated as follows:

$$T_*(|\Phi^\pm\rangle) = \frac{2\lambda}{\sqrt{5}\gamma} - \frac{2}{5\gamma}\ln(1 + \lambda),$$

$$T_*(|\Psi^+\rangle) = \frac{\lambda}{2\gamma} - \frac{1}{4\gamma}\ln(1 + 2\lambda),$$

and $T_*(|\Psi^-\rangle) \to \infty$ because $\mathcal{A} = 0$. This corresponds to the fact that the initial state $|\Psi^-\rangle$ does not change because it is identical to the zero eigenstate of M. Hence, as an information resource, $|\Psi^-\rangle$ is the best initial state against M. Also, as shown in Fig. 2(a), the set of states from $|\Psi^+\rangle$ spreads faster than that of $|\Phi^\pm\rangle$ as γ increases, implying that $|\Phi^\pm\rangle$ can preserve its coherence longer than $|\Psi^+\rangle$.

Next, we consider a qutrit, which is a symmetric two-qubit system described by a three-level system consisting of the distinguishable states $|E\rangle = [1, 0, 0]^\top$, $|S\rangle = [0, 1, 0]^\top$, and $|G\rangle = [0, 0, 1]^\top$. Note that $|S\rangle$ corresponds to the entangled state between two states. As seen in the qubit example, we investigate a reachable set of the target 3×3 gate. Let us consider a rotation operator of the three-dimensional system $G(\alpha, \beta, \delta) = R_z(\delta)R_y(\beta)R_x(\alpha)$, where matrix representations of R_i $(i = x, y, z)$ are given as

$$R_x(\alpha) = \begin{bmatrix} \cos\alpha & -\sin\alpha & 0 \\ \sin\alpha & \cos\alpha & 0 \\ 0 & 0 & 1 \end{bmatrix},$$

$$R_y(\beta) = \begin{bmatrix} \cos\beta & 0 & \sin\beta \\ 0 & 1 & 0 \\ -\sin\beta & 0 & \cos\beta \end{bmatrix},$$

$$R_z(\delta) = \begin{bmatrix} 1 & 0 & 0 \\ 0 & \cos\delta & -\sin\delta \\ 0 & \sin\delta & \cos\delta \end{bmatrix},$$

where α, β, and δ are the rotation angles about the x, y, and z axes. We limit the initial pure state to the real vector

$$|\psi_0\rangle = [\sin(\theta/2)\cos(\varphi/2),\ \cos(\theta/2),\ \sin(\theta/2)\sin(\varphi/2)]^\top,$$

where $0 \leqslant \theta, \varphi \leqslant \pi$. Also we assign the following Hamiltonian:

$$H_t = \Omega S_x + u_t S_z, \tag{11}$$

where $S_x = (|S\rangle\langle E| + |G\rangle\langle S|)/\sqrt{2}$+H.c., $S_y = i(|S\rangle\langle E| + |G\rangle\langle S|)/\sqrt{2}$+H.c., and $S_z = |E\rangle\langle E| - |G\rangle\langle G|$ are the spin angular momentum operators. This Hamiltonian is a straightforward extension of expression (8). Now, for instance, we choose $\delta = 0$ and $|\psi_0\rangle = (|E\rangle + |G\rangle)/\sqrt{2}$ at $(\theta, \varphi) = (\pi, \pi/2)$. In this setting, we obtain the lower bound as

$$T \geqslant T_* = \frac{\sqrt{1 - \cos\Theta_T}}{\Omega + u_{\max}}, \tag{12}$$

with

$$\cos\Theta_T = \tfrac{1}{4}(\cos\alpha\cos\beta + \cos\alpha\sin\beta + \cos\beta - \sin\beta)^2. \tag{13}$$

From Eq. (13), T_* is maximized when (α, β) satisfies $\cos\alpha = (\sin\beta - \cos\beta)/(\sin\beta + \cos\beta)$ [Fig. 2(b)]; here we typically take the following target gates:

$$G(\pi, 0) = \begin{bmatrix} -1 & 0 & 0 \\ 0 & -1 & 0 \\ 0 & 0 & 1 \end{bmatrix},\ G(0, \pi/2) = \begin{bmatrix} 0 & 0 & 1 \\ 0 & 1 & 0 \\ -1 & 0 & 0 \end{bmatrix},$$

$$G(\pi, \pi) = \begin{bmatrix} 1 & 0 & 0 \\ 0 & -1 & 0 \\ 0 & 0 & -1 \end{bmatrix}.$$

As noted in the previous section, the final states generated by the above gates are orthogonal to $|\psi_0\rangle$. Thus, it takes the longest to implement these G. Moreover, let us particularly consider the spin-up transformation $|\psi_0\rangle \to |E\rangle$, which is realized by $G(0, \pi/4)$ or $G(\pi, 3\pi/4)$. From Fig. 2(b), it is immediately found that this transformation takes $T = 0.45$ at least. In this way, we can roughly estimate the time to implement the target gate without solving any equations.

IV. CONCLUSION

Motivated by the work in Ref. [22], in this paper we have characterized the reachable set of Markovian open quantum systems under a given control setting based on the QSL. In order to make this analysis tractable and rigorous, it is important that the QSL is explicitly computable and tighter than other bounds; the QSL used in this paper indeed satisfies these conditions. Thanks to these features, as shown in Sec. III, we can clarify the set of all final states in a given control time and roughly estimate the time the controlled state exists in a certain region from the initial state without solving any equations. Important remaining work is to extend this approach to more strategic control cases, e.g., the measurement-based feedback control.

ACKNOWLEDGMENTS

This work was supported by MEXT Quantum Leap Flagship Program Grants No. JPMXS0118067285 and No. JPMXS0120319794.

APPENDIX A: PROOF OF QSL

We begin with taking the time derivative of Θ_t:

$$\begin{aligned} \frac{d\Theta_t}{dt} &= \frac{-1}{\sqrt{1 - \mathrm{Tr}(\rho_0\rho_t)^2}}\mathrm{Tr}\left(\rho_0\frac{d\rho_t}{dt}\right) \\ &= \frac{1}{\sin\Theta_t}\mathrm{Tr}\{(i[\rho_0, H] - \mathcal{D}^\dagger[M]\rho_0)\rho_t\}. \end{aligned} \tag{A1}$$

To have an upper bound of the right side of (A1), we often use the Schwarz inequality for matrices X and Y:

$$|\mathrm{Tr}(X^\dagger Y)| \leqslant \|X\|_{\mathrm{F}}\|Y\|_{\mathrm{F}}. \tag{A2}$$

Also the following inequality is often used:

$$\begin{aligned} \|\rho_t - \rho_0\|_{\mathrm{F}} &= \sqrt{\mathrm{Tr}[(\rho_t - \rho_0)^2]} = \sqrt{\mathrm{Tr}\left(\rho_t^2 - 2\rho_t\rho_0 + \rho_0^2\right)} \\ &\leqslant \sqrt{2 - 2\mathrm{Tr}(\rho_t\rho_0)} = \sqrt{2 - 2\cos\Theta_t}, \end{aligned}$$

where $\mathrm{Tr}(\rho_t^2) \leqslant 1$ and $\mathrm{Tr}(\rho_0^2) = 1$ are used. Using these inequalities, the right side of (A1) can be upper bounded as follows:

$$\begin{aligned} &\mathrm{Tr}\{(i[\rho_0, H] - \mathcal{D}^\dagger[M]\rho_0)\rho_t\} \\ &= \mathrm{Tr}\{(i[\rho_0, H] - \mathcal{D}^\dagger[M]\rho_0)(\rho_t - \rho_0)\} - \mathrm{Tr}(\rho_0\mathcal{D}^\dagger[M]\rho_0) \\ &= \mathrm{Tr}\{(i[H, \rho_0] + \mathcal{D}^\dagger[M]\rho_0)(\rho_0 - \rho_t)\} + \mathrm{Tr}(M^\dagger M\rho_0) \\ &\quad - \mathrm{Tr}(M^\dagger\rho_0 M\rho_0) \\ &\leqslant \|i[H, \rho_0] + \mathcal{D}^\dagger[M]\rho_0\|_{\mathrm{F}}\|\rho_t - \rho_0\|_{\mathrm{F}} + \|M|\psi_0\rangle\|^2 \\ &\quad - |\langle\psi_0|M|\psi_0\rangle|^2 \\ &\leqslant \sqrt{2}\|i[H, \rho_0] + \mathcal{D}^\dagger[M]\rho_0\|_{\mathrm{F}}\sqrt{1 - \cos\Theta_t} + \|M|\psi_0\rangle\|^2 \\ &\quad - |\langle\psi_0|M|\psi_0\rangle|^2 \\ &\leqslant \sqrt{2}(\|i[H, \rho_0] + \mathcal{D}^\dagger[M]\rho_0\|_{\mathrm{F}})\sqrt{1 - \cos\Theta_t} \\ &\quad + \|M|\psi_0\rangle\|^2 - |\langle\psi_0|M|\psi_0\rangle|^2 \\ &= \mathcal{A}\sqrt{1 - \cos\Theta_t} + \mathcal{E}, \end{aligned} \tag{A3}$$

where we have defined

$$\mathcal{A} = \sqrt{2}(\|i[H, \rho_0] + \mathcal{D}^\dagger[M]\rho_0\|_{\mathrm{F}}),$$
$$\mathcal{E} = \|M|\psi_0\rangle\|^2 - |\langle\psi_0|M|\psi_0\rangle|^2.$$

Combining Eqs. (A1) and (A3), we have

$$\frac{d\Theta_t}{dt} \leqslant \frac{1}{\sin\Theta_t}(\mathcal{A}\sqrt{1-\cos\Theta_t} + \mathcal{E}). \tag{A4}$$

By integrating (A4) from $t = 0$ to T, we straightforwardly end up with the lower bound

$$T \geqslant T_* := \frac{2\lambda}{\mathcal{A}} + \frac{2\mathcal{E}}{\mathcal{A}^2}\ln\left(\frac{\mathcal{E}}{\mathcal{E}+\mathcal{A}\lambda}\right). \tag{A5}$$

APPENDIX B: COMPARISON BETWEEN THE EXACT EVOLUTION TIME AND QSL

Here to show the actual tightness of the lower bound T_*, let us compare T_* with the exact evolution time T from the initial state to the final state with simple settings.

First, we consider the case where the closed system $|\psi_t\rangle = [\cos\theta_t, \sin\theta_t]^\top$ is driven only by the time-independent Hamiltonian $H = \Omega\sigma_y$ ($M = 0$) from $|\psi_0\rangle = |1\rangle$ to $|\psi_T\rangle = |0\rangle$. In this case, by solving the equation $d|\psi_t\rangle/dt = -i\Omega\sigma_y|\psi_t\rangle$, we have $\theta_t = \Omega t + \pi/2$. Then the exact solution T is given by

$$T = \frac{\arcsin(\lambda)}{\Omega},$$

and $T_* = \lambda/\Omega$. Figure 3(a) shows T and T_* with $\Omega = 1$ as a function of λ. We find that T_* works as a tighter bound when λ is small; that is, when ΩT is small, the theoretical upper bound $\Omega T \geqslant \lambda$ is tight.

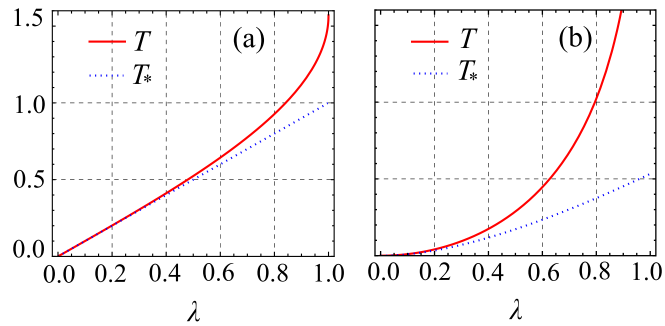

FIG. 3. Comparison of the exact evolution time T (solid red line) and its lower bound T_* (dotted blue line) as a function of λ for (a) $\Omega = 1$ and (b) $\gamma = 1$.

Next, we set $H = 0$ and $M = \sqrt{\gamma}\sigma_-$ and choose the initial state $|\psi_0\rangle = |0\rangle$. In this case, the master equation $d\rho_t = \mathcal{D}[M]\rho_t$ yields a solution $\cos\Theta_T = e^{-\gamma T}$. As a result, we obtain

$$T = -\frac{1}{\gamma}\ln(1-\lambda^2),\ T_* = \frac{\sqrt{2}\lambda}{\gamma} - \frac{1}{\gamma}\ln(1+\sqrt{2}\lambda).$$

Like the result shown in Fig. 3(a), T_* gives a tighter bound when λ is small [Fig. 3(b)], where the range of the vertical axis is the same as that in Fig. 3(a). However, as λ increases, the gap between T and T_* becomes bigger more quickly than that in Fig. 3(a).

[1] G. Dirr, U. Helmke, I. Kurniawan, and T. Schlte-Herbruggen, Lie-semigroup structures for reachability and control of open quantum systems: Kossakowski-Lindblad generators form lie wedge to Markovian channels, Rep. Math. Phys. **64**, 93 (2009).

[2] G. Dirr, U. Helmke, M. Kleinsteuber, S. Glaser, and T. Schulte-Herbrüggen, The local C-numerical range: Examples, conjectures, and numerical algorithms, *Proc. MTNS, Kyoto, Japan* (2006).

[3] H. Yuan, Reachable set of operators on controlled open quantum systems in a Markovian environment, Automatica **49**, 955 (2013).

[4] L. Mandelstam and I. Tamm, The uncertainty relation between energy and time in nonrelativistic quantum mechanics, J. Phys. (USSR) **9**, 249 (1945).

[5] N. Margolus and L. B. Levitin, The maximum speed of dynamical evolution, Phys. D (Amsterdam, Neth.) **120**, 188 (1998).

[6] A. Uhlmann, An energy dispersion estimate, Phys. Lett. A **161**, 329 (1992).

[7] V. Giovannetti, S. Lloyd, and L. Maccone, Quantum limits to dynamical evolution, Phys. Rev. A **67**, 052109 (2003).

[8] S. Luo and Z. Zhang, On decaying rate of quantum states, Lett. Math. Phys. **71**, 1 (2005).

[9] P. Pfeifer, How Fast can a Quantum State Change with Time? Phys. Rev. Lett. **70**, 3365 (1993).

[10] P. Pfeifer and J. Frohlich, Generalized time-energy uncertainty relations and bounds on lifetimes of resonance, Rev. Mod. Phys. **67**, 759 (1995).

[11] M. M. Taddei, B. M. Escher, L. Davidovich, and R. L. de Matos Filho, Quantum Speed Limit for Physical Processes, Phys. Rev. Lett. **110**, 050402 (2013).

[12] A. del Campo, I. L. Egusquiza, M. B. Plenio, and S. F. Huelga, Quantum Speed Limits in Open System Dynamics, Phys. Rev. Lett. **110**, 050403 (2013).

[13] S. Deffner and E. Lutz, Quantum Speed Limit for Non-Markovian Dynamics, Phys. Rev. Lett. **111**, 010402 (2013).

[14] Z. Sun, J. Liu, J. Ma, and X. Wang, Quantum speed limits in open systems: Non-Markovian dynamics without rotating-wave approximation, Sci. Rep. **5**, 8444 (2015).

[15] X. Meng, C. Wu, and H. Guo, Minimal evolution time and quantum speed limit of non-Markovian open systems, Sci. Rep. **5**, 16357 (2015).

[16] Y.-J. Zhang, W. Han, Y.-J. Xia, J.-P. Cao, and H. Fan, Quantum speed limit for arbitrary initial states, Sci. Rep. **6**, 27349 (2016).

[17] T. Caneva, M. Murphy, T. Calarco, R. Fazio, S. Montangero, V. Giovannetti, and G. E. Santoro, Optimal Control at the Quantum Speed Limit, Phys. Rev. Lett. **103**, 240501 (2009).

[18] P. M. Poggi, F. C. Lombardo, and D. A. Wisniacki, Quantum speed limit and optimal evolution time in a two-level system, Europhys. Lett. **104**, 40005 (2013).
[19] O. Andersson and H. Heydari, Quantum speed limits and optimal Hamiltonians for driven systems in mixed states, J. Phys. A **47**, 215301 (2014).
[20] P. M. Poggi, Geometric quantum speed limits and short-time accessibility to unitary operations, Phys. Rev. A **99**, 042116 (2019).
[21] P. M. Poggi, Analysis of lower bounds for quantum control times and their relation to the quantum speed limit, An. AFA **31**, 29 (2020).
[22] C. Arenz, B. Russell, D. Burgarth, and H. Rabitz, The roles of drift and control field constraints upon quantum control speed limits, New J. Phys. **19**, 103015 (2017).
[23] K. Kobayashi and N. Yamamoto, Quantum speed limit for robust state characterization and engineering, Phys. Rev. A **102**, 042606 (2020).